Smart Structures and Systems, *Vol. 18, No. 2 (2016) 267-291*
DOI: http://dx.doi.org/10.12989/sss.2016.18.2.267

Thermal buckling response of functionally graded sandwich plates with clamped boundary conditions

Zohra Abdelhak[1,2], Lazreg Hadji*[2,3], T. Hassaine Daouadji[2,3] and E.A. Adda Bedia[2]

[1]Université Ahmed Zabana, R Bourmadia, 48000 Relizane, Algérie
[2]Laboratoire des Matériaux & Hydrologie, Université de Sidi Bel Abbes, 22000 Sidi Bel Abbes, Algérie
[3]Université Ibn Khaldoun, BP 78 Zaaroura, 14000 Tiaret, Algérie

(Received November 27, 2015, Revised May 20, 2016, Accepted May 20, 2016)

Abstract. In this research work, an exact analytical solution for thermal buckling analysis of functionally graded material (FGM) sandwich plates with clamped boundary condition subjected to uniform, linear, and non-linear temperature rises across the thickness direction is developed. Unlike any other theory, the number of unknown functions involved is only four, as against five in case of other shear deformation theories. The theory accounts for parabolic distribution of the transverse shear strains, and satisfies the zero traction boundary conditions on the surfaces of the plate without using shear correction factor. A power law distribution is used to describe the variation of volume fraction of material compositions. Equilibrium and stability equations are derived based on the present refined theory. The non-linear governing equations are solved for plates subjected to simply supported and clamped boundary conditions. The thermal loads are assumed to be uniform, linear and non-linear distribution through-the-thickness. The effects of aspect and thickness ratios, gradient index, on the critical buckling are all discussed.

Keywords: functionally graded plates; refined theory; sandwich plate; clamped boundary conditions; thermal buckling

1. Introduction

Functionally graded materials (FGMs) are new inhomogeneous materials which have widely used in many engineering applicants such as nuclear reactors and high-speed spacecraft industries (Yamanouchi 1990). The mechanical properties of FGMs vary smoothly and continuously from one surface to the other. Typically these materials are made from a mixture of ceramic and metal or from a combination of different materials. The ceramic constituent of the material provides the high-temperature resistance due to its low thermal conductivity. The ductile metal constituent on the other hand, prevents fracture caused by stresses due to the high temperature gradient in a very short period of time. Furthermore a mixture of ceramic and metal with a continuously varying volume fraction can be easily manufactured (Fukui 1991, Koizumi 1997). With the developments in manufacturing methods (Fukui 1991, Fukui 1997, El-Hadek 2003) functionally graded materials

*Corresponding author, Dr., E-mail: had_laz@yahoo.fr

http://www.techno-press.org/?journal=sss&subpage=8 ISSN: 1738-1584 (Print), 1738-1991 (Online)

seem to have great potential in sandwich structures. The analysis of these materials has been considered by many researchers. Due to the importance and wide engineering applications of FGMs, the static, vibrational, thermomechanical and buckling analyses of FGM structures have been addressed by many investigators.

The functionally graded (FG) plates are commonly used in thermal environments; they can buckle under thermal and mechanical loads. Thus, the buckling analysis of such plates is essential to ensure an efficient and reliable design. Eslami and his co-workers (Javaheri (2002), Javaheri and Eslami (2002), Samsam and Eslami (2007), Javaheri and Eslami (2005), Samsam and Eslami (2006), Samsam and Eslami (2005) have treated a series of problems relating to the linear buckling of simply supported rectangular FG plates, with and without imperfections, under mechanical and thermal loads. By using an analytical approach, they obtained closed-form expressions for buckling loads.

Sohn and Kim (2008) dealt with the stabilities of FG panels subjected to combined thermal and aerodynamic loads. The first-order theory was used to simulate supersonic aerodynamic loads acting on the panels. The influence of the material constitution of FG panels on thermal buckling and flutter characteristics was examined. Zenkour *et al.* (2010) studied the thermal buckling response of FG plates using sinusoidal shear deformation plate theory. Bouiadjra *et al.* (2012) developed a four-variable refined plate theory for buckling analysis of functionally graded plates. Xiang *et al.* (2013) used a n-order four variable refined theory for bending and free vibration of functionally graded plates. Recently, Tounsi and his co-workers workers (Tounsi *et al*. 2013, Ait Yahia *et al*. 2015, Zidi *et al.* 2014, Bouderba *et al.* 2013, Bellifa *et al.* 2016, Atia *et al.* 2015, Bouchafa, *et al.* 2015) developed new shear deformation plates theories involving only four unknown functions. Ait Amar Meziane *et al.* (2014) developed an efficient and simple refined theory for buckling and free vibration of exponentially graded sandwich plates under various boundary conditions. Mahi *et al.* (2015) studied the bending and free vibration analysis of isotropic, functionally graded, sandwich and laminated composite plates using a new hyperbolic shear deformation theory. Bourada *et al.* (2015) used a new simple shear and normal deformations theory for functionally graded beams. Belabed *et al*. (2014) used an efficient and simple higher order shear and normal deformation theory for functionally graded material (FGM) plates. Hebali *et al.* (2014) studied the static and free vibration analysis of functionally graded plates using a new quasi-3D hyperbolic shear deformation theory. Hamidi *et al.* (2015) used a sinusoidal plate theory with 5-unknowns and stretching effect for thermomechanical bending of functionally graded sandwich plates. Bennoun *et al.* (2016) studied the vibration analysis of functionally graded sandwich plates using a novel five variable refined plate theory. Bousahla *et al*. (2014) investigated a novel higher order shear and normal deformation theory based on neutral surface position for bending analysis of advanced composite plates.

In this paper, the four-variable refined plate theory has been extended for the first time to the thermal buckling behavior of FGM sandwich plates with clamped boundary condition. Material properties of the FGM sandwich plate are assumed to vary in the thickness direction according to a simple power-law distribution in terms of the volume fractions of the constituents. An eigenvalue problem is formulated for a FGM sandwich plates to analyze its thermal buckling behaviors. The thermal loads are assumed as uniform, linear, and nonlinear temperature rises across the thickness direction. Illustrative examples are given so as to demonstrate the efficacies of the theory. The effects of various variables, such as thickness and aspect ratios, gradient index, loading type, and sandwich plate type on the critical buckling are all discussed.

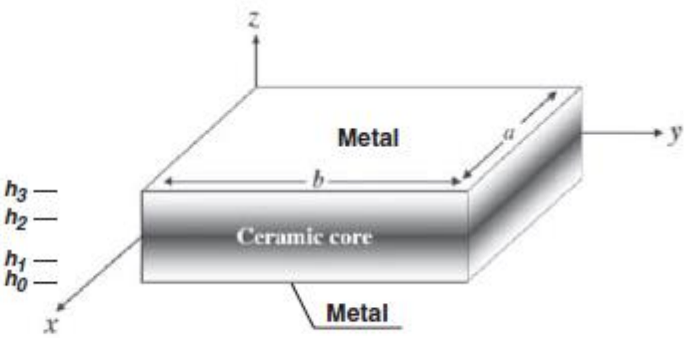

Fig. 1 Geometry of the functionally graded material (FGM) sandwich plate

2. Statement of the problem

The geometry and dimensions of the rectangular plate made of FGMs under consideration are represented in Fig. 1. Rectangular Cartesian coordinates (x, y, z) are used to describe infinitesimal deformations of a three-layer sandwich elastic plate occupying the region $[0,a]\times[0,b]\times[-h/2,h/2]$ in the unstressed reference configuration, and the axes are parallel to the edges of the plate. The plate has length a, width b, and uniform thickness h. The mid-plane of the composite sandwich plate is defined by $z=0$ and its external bounding planes being defined by $z=\pm h/2$. The vertical positions of the bottom surface, the two interfaces between the core and faces layers, and the top surface are denoted, respectively, by $h_0 = -h/2$, h_1, h_2, and $h_3 = +h/2$.

The effective material properties for each layer, such as Young's modulus, Poisson's ratio, and thermal expansion coefficient, can be expressed as

$$P^{(n)}(z) = P_m + (P_c - P_m)V^{(n)} \tag{1}$$

where $P^{(n)}$ is the effective material property of FGM of layer n. P_m and P_c denote the property of the bottom and top faces of layer 1. $(h_0 \le z \le h_1)$, respectively, and vice versa for layer 3 $(h_2 \le z \le h_3)$ depending on the volume fraction $V^{(n)}(n=1,2,3)$. Note that P_m and P_c are, respectively, the corresponding properties of the metal and ceramic of the FGM sandwich plate. The volume fraction $V^{(n)}$ of the FGMs is assumed to obey a power-law function along the thickness direction (Houari *et al*. (2011))

$$V^{(1)} = \left(\frac{z-h_1}{h_2-h_1}\right)^k, \; z\in[h_1,h_2] \tag{2a}$$

$$V^{(2)} = 1, \; z\in[h_2,h_3] \tag{2b}$$

$$V^{(3)} = \left(\frac{z - h_4}{h_3 - h_4} \right)^k, \ z \in [h_3, h_4] \tag{2c}$$

where k is the volume fraction exponent, which takes values greater than or equals to zero. The core layer is independent of the value of k, which is a fully ceramic layer. However, the value of k equal to zero represents a fully ceramic plate. The above power-law assumption given in Eqs. (2(a)) and (2(c)) reflects a simple rule of mixtures used to obtain the effective properties of the metal–ceramic and ceramic–metal plate faces (see Fig. 1). Note that the volume fraction of the metal is high near the bottom and top surfaces of the plate and that of ceramic is high near the interfaces.

3. Basic assumptions

Assumptions of the present theory are as follows:

- The displacements are small in comparison with the plate thickness and, therefore, s trains involved are infinitesimal.
- The transverse displacement w includes two components of bending w_b and shear w_s. These components are functions of coordinates x, y only.

$$w(x, y, z) = w_b(x, y) + w_s(x, y) \tag{3}$$

- The transverse normal stress σ_z is negligible in comparison with in-plane σ_x and σ_y.
- The displacements u in x-direction and v in y-direction consist of extension, ben ding, and shear components.

$$u = u_0 + u_b + u_s, \ v = v_0 + v_b + v_s, \tag{4}$$

The bending components u_b and v_b are assumed to be similar to the displacements given by the classical plate theory. Therefore, the expression for u_b and v_b can be given as

$$u_b = -z \frac{\partial w_b}{\partial x}, \qquad v_b = -z \frac{\partial w_b}{\partial y} \tag{5}$$

The shear components u_s and v_s give rise, in conjunction with w_s, to the sinusoidal variations of shear strains γ_{xz}, γ_{yz} and hence to shear stresses τ_{xz}, τ_{yz} through the thickness of the plate in such a way that shear stresses τ_{xz}, τ_{yz} are zero at the top and bottom faces of the plate. Consequently, the expression for u_s and v_s can be given as

$$u_s = -f(z) \frac{\partial w_s}{\partial x}, \quad v_s = -f(z) \frac{\partial w_s}{\partial y} \tag{6}$$

where

$$f(z) = z - \frac{1}{2} z \left(\frac{1}{4} h^2 - \frac{1}{3} z^2 \right) \tag{7}$$

4. Kinematics and constitutive equations

Based on the assumptions made in the preceding section, the displacement field can be obtained using Eqs. (3)- (7) as

$$u(x,y,z) = u_0(x,y) - z\frac{\partial w_b}{\partial x} - f(z)\frac{\partial w_s}{\partial x}$$

$$v(x,y,z) = v_0(x,y) - z\frac{\partial w_b}{\partial y} - f(z)\frac{\partial w_s}{\partial y} \tag{8}$$

$$w(x,y,z) = w_b(x,y) + w_s(x,y)$$

The non-linear von Karman strain–displacement equations are as follows

$$\begin{Bmatrix} \varepsilon_x \\ \varepsilon_y \\ \gamma_{xy} \end{Bmatrix} = \begin{Bmatrix} \varepsilon_x^0 \\ \varepsilon_y^0 \\ \gamma_{xy}^0 \end{Bmatrix} + z \begin{Bmatrix} k_x^b \\ k_y^b \\ k_{xy}^b \end{Bmatrix} + f(z) \begin{Bmatrix} k_x^s \\ k_y^s \\ k_{xy}^s \end{Bmatrix}, \quad \begin{Bmatrix} \gamma_{yz} \\ \gamma_{xz} \end{Bmatrix} = g(z) \begin{Bmatrix} \gamma_{yz}^0 \\ \gamma_{xz}^0 \end{Bmatrix} \tag{9}$$

Where

$$\begin{Bmatrix} \varepsilon_x^0 \\ \varepsilon_y^0 \\ \gamma_{xy}^0 \end{Bmatrix} = \begin{Bmatrix} \dfrac{\partial u_0}{\partial x} + \dfrac{1}{2}\left(\dfrac{\partial w_b}{\partial x} + \dfrac{\partial w_s}{\partial x} \right)^2 \\ \dfrac{\partial v_0}{\partial y} + \dfrac{1}{2}\left(\dfrac{\partial w_b}{\partial y} + \dfrac{\partial w_s}{\partial y} \right)^2 \\ \dfrac{\partial u_0}{\partial y} + \dfrac{\partial v_0}{\partial x} + \left(\dfrac{\partial w_b}{\partial x} + \dfrac{\partial w_s}{\partial x} \right)\left(\dfrac{\partial w_b}{\partial y} + \dfrac{\partial w_s}{\partial y} \right) \end{Bmatrix}$$

$$\begin{Bmatrix} k_x^b \\ k_y^b \\ k_{xy}^b \end{Bmatrix} = \begin{Bmatrix} -\dfrac{\partial^2 w_b}{\partial x^2} \\ -\dfrac{\partial^2 w_b}{\partial y^2} \\ -2\dfrac{\partial^2 w_b}{\partial x \partial y} \end{Bmatrix}, \begin{Bmatrix} k_x^s \\ k_y^s \\ k_{xy}^s \end{Bmatrix} = \begin{Bmatrix} -\dfrac{\partial^2 w_s}{\partial x^2} \\ -\dfrac{\partial^2 w_s}{\partial y^2} \\ -2\dfrac{\partial^2 w_s}{\partial x \partial y} \end{Bmatrix} \tag{10.a}$$

$$\begin{Bmatrix} \gamma_{yz}^0 \\ \gamma_{xz}^0 \end{Bmatrix} = \begin{Bmatrix} \dfrac{\partial w_s}{\partial y} \\ \dfrac{\partial w_s}{\partial x} \end{Bmatrix}$$

and

$$g(z) = 1 - \frac{d\, f(z)}{d\, z} \tag{10b}$$

For elastic and isotropic FGMs, the constitutive relations can be written as

$$\begin{Bmatrix} \sigma_x \\ \sigma_y \\ \tau_{xy} \end{Bmatrix}^{(n)} = \begin{bmatrix} Q_{11} & Q_{12} & 0 \\ Q_{12} & Q_{22} & 0 \\ 0 & 0 & Q_{66} \end{bmatrix}^{(n)} \begin{Bmatrix} \varepsilon_x - \alpha T \\ \varepsilon_y - \alpha T \\ \gamma_{xy} \end{Bmatrix}^{(n)} \quad \begin{Bmatrix} \tau_{yz} \\ \tau_{zx} \end{Bmatrix}^{(n)} = \begin{bmatrix} Q_{44} & 0 \\ 0 & Q_{55} \end{bmatrix}^{(n)} \begin{Bmatrix} \gamma_{yz} \\ \gamma_{zx} \end{Bmatrix}^{(n)} \tag{11}$$

where (σ_x , σ_y , τ_{xy} , τ_{yz} , τ_{yx}) and (ε_x , ε_y , γ_{xy} , γ_{yz} , γ_{xz}) are the stress and strain components, respectively. Using the material properties defined in Eq. (1), stiffness coefficients, Q_{ij} , can be expressed as

$$Q_{11}^n = Q_{22}^n = \frac{E^{(n)}(z)}{1-\nu^2}, \tag{12a}$$

$$Q_{12}^{(n)} = \frac{\nu\, E^{(n)}(z)}{1-\nu^2}, \tag{12b}$$

$$Q_{44}^{(n)} = Q_{55}^{(n)} = Q_{66}^{(n)} = \frac{E^{(n)}(z)}{2(1+\nu)}, \tag{12c}$$

5. Stability equations

The total potential energy of the FG plate may be written as

$$U = \frac{1}{2}\iiint\left[\sigma_x\left(\varepsilon_x - \alpha T\right) + \sigma_y\left(\varepsilon_y - \alpha T\right) + \tau_{xy}\gamma_{xy} + \tau_{yz}\gamma_{yz} + \tau_{xz}\gamma_{xz}\right]dx\,dy\,dz \tag{13}$$

The principle of virtual work for the present problem may be expressed as follows

$$\iint\left[\begin{array}{l} N_x\delta\varepsilon_x^0 + N_y\delta\varepsilon_y^0 + N_{xy}\delta\gamma_{xy}^0 + M_x^b\delta k_x^b + M_y^b\delta k_y^b + M_{xy}^b\delta k_{xy}^b + M_x^s\delta k_x^s \\ + M_y^s\delta k_y^s + M_{xy}^s\delta k_{xy}^s + S_{yz}^s\delta\gamma_{yz}^s + S_{xz}^s\delta\gamma_{xz}^s \end{array}\right]dx\,dy = 0 \tag{14}$$

where

$$\begin{Bmatrix} N_x & N_y & N_{xy} \\ M_x^b & M_y^b & M_{xy}^b \\ M_x^s & M_y^s & M_{xy}^s \end{Bmatrix} = \sum_{n=1}^{3}\int_{h_{n-1}}^{h_n}\left(\sigma_x, \sigma_y, \tau_{xy}\right)\begin{Bmatrix} 1 \\ z \\ f(z) \end{Bmatrix}dz \tag{15a}$$

$$\left(S_{xz}^s, S_{yz}^s\right) = \sum_{n=1}^{3}\int_{h_{n-1}}^{h_n}\left(\tau_{xz}, \tau_{yz}\right)g(z)dz \tag{15b}$$

where h_n and h_{n-1} are the top and bottom z-coordinates of the nth layer.
Using Eq. (13) in Eq. (15), the stress resultants of the FG plate can be related to the total strains by

$$\begin{Bmatrix} N \\ M^b \\ M^s \end{Bmatrix} = \begin{bmatrix} A & B & B^s \\ B & D & D^s \\ B^s & D^s & H^s \end{bmatrix}\begin{Bmatrix} \varepsilon \\ k^b \\ k^s \end{Bmatrix} - \begin{Bmatrix} N^T \\ M^{bT} \\ M^{sT} \end{Bmatrix}, \qquad S = A^s\gamma \tag{16}$$

Where

$$N = \left\{N_x, N_y, N_{xy}\right\}^t,\; M^b = \left\{M_x^b, M_y^b, M_{xy}^b\right\}^t,\; M^s = \left\{M_x^s, M_y^s, M_{xy}^s\right\}^t, \tag{17a}$$

$$N^T = \left\{N_x^T, N_y^T, 0\right\}^t,\; M^{bT} = \left\{M_x^{bT}, M_y^{bT}, 0\right\}^t,\; M^{sT} = \left\{M_x^{sT}, M_y^{sT}, 0\right\}^t, \tag{17b}$$

$$\varepsilon = \left\{\varepsilon_x^0, \varepsilon_y^0, \gamma_{xy}^0\right\}^t,\; k^b = \left\{k_x^b, k_y^b, k_{xy}^b\right\}^t,\; k^s = \left\{k_x^s, k_y^s, k_{xy}^s\right\}^t, \tag{17c}$$

$$A = \begin{bmatrix} A_{11} & A_{12} & 0 \\ A_{12} & A_{22} & 0 \\ 0 & 0 & A_{66} \end{bmatrix},\; B = \begin{bmatrix} B_{11} & B_{12} & 0 \\ B_{12} & B_{22} & 0 \\ 0 & 0 & B_{66} \end{bmatrix},\; D = \begin{bmatrix} D_{11} & D_{12} & 0 \\ D_{12} & D_{22} & 0 \\ 0 & 0 & D_{66} \end{bmatrix} \tag{17d}$$

$$B^s = \begin{bmatrix} B_{11}^s & B_{12}^s & 0 \\ B_{12}^s & B_{22}^s & 0 \\ 0 & 0 & B_{66}^s \end{bmatrix},\; D^s = \begin{bmatrix} D_{11}^s & D_{12}^s & 0 \\ D_{12}^s & D_{22}^s & 0 \\ 0 & 0 & D_{66}^s \end{bmatrix},\; H^s = \begin{bmatrix} H_{11}^s & H_{12}^s & 0 \\ H_{12}^s & H_{22}^s & 0 \\ 0 & 0 & H_{66}^s \end{bmatrix} \tag{17e}$$

$$S = \left\{ S_{xz}^s, S_{yz}^s \right\}^t, \; \gamma = \left\{ \gamma_{xz}^s, \gamma_{yz}^s \right\}^t, \; A^s = \begin{bmatrix} A_{44}^s & 0 \\ 0 & A_{55}^s \end{bmatrix}, \tag{17f}$$

where A_{ij}, B_{ij}, etc., are the plate stiffness, defined by

$$\begin{Bmatrix} A_{11} & B_{11} & D_{11} & B_{11}^s & D_{11}^s & H_{11}^s \\ A_{12} & B_{12} & D_{12} & B_{12}^s & D_{12}^s & H_{12}^s \\ A_{66} & B_{66} & D_{66} & B_{66}^s & D_{66}^s & H_{66}^s \end{Bmatrix} = \sum_{n=1}^{3} \int_{h_{n-1}}^{h_n} \left(1, z, z^2, f(z), zf(z), f^2(z)\right) \begin{Bmatrix} 1 \\ \nu^{(n)} \\ \dfrac{1-\nu^{(n)}}{2} \end{Bmatrix} dz, \tag{18a}$$

and

$$\left(A_{22}, B_{22}, D_{22}, B_{22}^s, D_{22}^s, H_{22}^s\right) = \left(A_{11}, B_{11}, D_{11}, B_{11}^s, D_{11}^s, H_{11}^s\right), \quad Q_{11}^{(n)} = \frac{E(z)}{1-\nu^2}, \tag{18b}$$

$$A_{44}^s = A_{55}^s = \sum_{n=1}^{3} \int_{h_{n-1}}^{h_n} \frac{E(z)}{2(1+\nu)} \left[g(z)\right]^2 dz, \tag{18c}$$

The stress and moment resultants, $N_x^T = N_y^T, M_x^{bT} = M_y^{bT}$ and $M_x^{sT} = M_y^{sT}$ due to thermal loading are defined by

$$\begin{Bmatrix} N_x^T \\ M_x^{bT} \\ M_x^{sT} \end{Bmatrix} = \sum_{n=1}^{3} \int_{h_{n-1}}^{h_n} \frac{E^{(n)}(z)}{1-\nu} \alpha^{(n)}(z) T \begin{Bmatrix} 1 \\ z \\ f(z) \end{Bmatrix} dz, \tag{19}$$

The stability equations of the plate may be derived by the adjacent equilibrium criterion. Assume that the equilibrium state of the FG plate under thermal loads is defined in terms of the displacement components $\left(u_0^0, v_0^0, w_b^0, w_s^0\right)$. The displacement components of a neighboring stable state differ by $\left(u_0^1, v_0^1, w_b^1, w_s^1\right)$ with respect to the equilibrium position. Thus, the total displacements of a neighboring state are

$$u_0 = u_0^0 + u_0^1, \; v_0 = v_0^0 + v_0^1, \; w_b = w_b^0 + w_b^1, \; w_s = w_s^0 + w_s^1, \tag{20}$$

Where the superscript 1 refers to the state of stability and the superscript 0 refers to the state of equilibrium conditions.

Substituting Eqs. (9) and (20) into Eq. (14) and integrating by parts and then equating the coefficients of $\delta u_0^1, \delta v_0^1, \delta w_b^1, \delta w_s^1$, to zero, separately, the governing stability equations are obtained for the shear deformation plate theories as

$$\begin{aligned}
&\frac{\partial N_x^1}{\partial x}+\frac{\partial N_{xy}^1}{\partial y}=0\\
&\frac{\partial N_{xy}^1}{\partial x}+\frac{\partial N_y^1}{\partial y}=0\\
&\frac{\partial^2 M_x^{b1}}{\partial x^2}+2\frac{\partial^2 M_{xy}^{b1}}{\partial x\partial y}+\frac{\partial^2 M_y^{b1}}{\partial y^2}+\overline{N}=0\\
&\frac{\partial^2 M_x^{s1}}{\partial x^2}+2\frac{\partial^2 M_{xy}^{s1}}{\partial x\partial y}+\frac{\partial^2 M_y^{s1}}{\partial y^2}+\frac{\partial S_{xz}^{s1}}{\partial x}+\frac{\partial S_{yz}^{s1}}{\partial y}+\overline{N}=0
\end{aligned} \tag{21}$$

with

$$\overline{N}=N_x^0\frac{\partial^2\left(w_b^1+w_s^1\right)}{\partial x^2}+N_y^0\frac{\partial^2\left(w_b^1+w_s^1\right)}{\partial y^2} \tag{22}$$

where the terms N_x^0 and N_y^0 are the pre-buckling force resultants obtained as

$$N_{cr}=N_x^0=N_y^0=-\sum_{n=1}^{3}\int_{h_{n-1}}^{h_n}\frac{\alpha(z)E(z)T}{1-\nu}dz. \tag{23}$$

The stability equations in terms of the displacement components may be obtained by substituting Eq. (16) into Eq. (21). The resulting equations are four stability equations based on the present refined shear deformation theory for FG plates.

$$\begin{aligned}
&A_{11}d_{11}u_0+A_{66}d_{22}u_0+\left(A_{12}+A_{66}\right)d_{12}v_0-B_{11}d_{111}w_b-\left(B_{12}+2B_{66}\right)d_{122}w_b\\
&\quad-\left(B_{12}^s+2B_{66}^s\right)d_{122}w_s-B_{11}^s d_{111}w_s=0,
\end{aligned} \tag{24a}$$

$$\begin{aligned}
&A_{22}d_{22}v_0+A_{66}d_{11}v_0+\left(A_{12}+A_{66}\right)d_{12}u_0-B_{22}d_{222}w_b-\left(B_{12}+2B_{66}\right)d_{112}w_b\\
&\quad-\left(B_{12}^s+2B_{66}^s\right)d_{112}w_s-B_{22}^s d_{222}w_s=0,
\end{aligned} \tag{24b}$$

$$\begin{aligned}
&B_{11}d_{111}u_0+\left(B_{12}+2B_{66}\right)d_{122}u_0+\left(B_{12}+2B_{66}\right)d_{112}v_0\\
&+B_{22}d_{222}v_0-D_{11}d_{1111}w_b-2\left(D_{12}+2D_{66}\right)d_{1122}w_b-D_{22}d_{2222}w_b\\
&-D_{11}^s d_{1111}w_s-2\left(D_{12}^s+2D_{66}^s\right)d_{1122}w_s-D_{22}^s d_{2222}w_s+N_{cr}=0
\end{aligned} \tag{24c}$$

$$\begin{aligned}
&B_{11}^s d_{111}u_0+\left(B_{12}^s+2B_{66}^s\right)d_{122}u_0+\left(B_{12}^s+2B_{66}^s\right)d_{112}v_0\\
&+B_{22}^s d_{222}v_0-D_{11}^s d_{1111}w_b-2\left(D_{12}^s+2D_{66}^s\right)d_{1122}w_b\\
&-D_{22}^s d_{2222}w_b-H_{11}^s d_{1111}w_s-2\left(H_{12}^s+2H_{66}^s\right)d_{1122}w_s\\
&-H_{22}^s d_{2222}w_s+A_{55}^s d_{11}w_s+A_{44}^s d_{22}w_s+N_{cr}=0
\end{aligned} \tag{24d}$$

where d_{ij}, d_{ijl}, and d_{ijlm} are the following differential operators

$$d_{ij} = \frac{\partial^2}{\partial x_i \partial x_j},\, d_{ijl} = \frac{\partial^3}{\partial x_i \partial x_j \partial x_l},\, d_{ijlm} = \frac{\partial^4}{\partial x_i \partial x_j \partial x_l \partial x_m},\, d_i = \frac{\partial}{\partial x_i},\quad (i, j, l, m = 1,2). \tag{25}$$

6. Trigonometric solution to thermal buckling

The exact solution of Eqs. (24) for the FGMs sandwich plate under various boundary conditions can be constructed. The boundary conditions for an arbitrary edge with simply supported and clamped edge conditions are:

- Clamped (C):

$$u_0 = v_0 = w_b = \partial w_b / \partial x = \partial w_b / \partial y = w_s = \partial w_s / \partial x = \partial w_s / \partial y = 0 \quad \text{à} \quad x = 0, a \;\; y = 0, b \tag{26}$$

- Simply Supported (S):

$$v_0 = w_b = \partial w_b / \partial y = w_s = \partial w_s / \partial y = 0 \quad \text{à} \quad x = 0, a \tag{27a}$$

$$u_0 = w_b = \partial w_b / \partial x = w_s = \partial w_s / \partial x = 0 \quad \text{à} \quad y = 0, b \tag{27b}$$

The following representation for the displacement quantities, that satisfy the above boundary conditions, is appropriate in the case of our problem

$$\begin{Bmatrix} u_0 \\ v_0 \\ w_b \\ w_s \end{Bmatrix} = \begin{Bmatrix} U_{mn} \dfrac{\partial X_m(x)}{\partial x} Y_n(y) \\ V_{mn} X_m(x) \dfrac{\partial Y_n(y)}{\partial y} \\ W_{bmn} X_m(x) Y_n(y) \\ W_{smn} X_m(x) Y_n(y) \end{Bmatrix} \tag{28}$$

Table 1 The admissible functions

	Boundary conditions		The functions X_m and Y_n	
	At $x = 0, a$	At $y = 0, b$	$X_m(x)$	$Y_n(y)$
SSSS	$X_m(0) = X_m''(0) = 0$	$Y_n(0) = Y_n''(0) = 0$	$\sin(\lambda\, x)$	$\sin(\mu\, y)$
	$X_m(a) = X_m''(a) = 0$	$Y_n(b) = Y_n''(b) = 0$		
	$X_m(a) = X_m'(a) = 0$	$Y_n(b) = Y_n''(b) = 0$		
CCCC	$X_m(0) = X_m'(0) = 0$	$Y_n(0) = Y_n''(0) = 0$	$\sin^2(\lambda\, x)$	$\sin^2(\mu\, y)$
	$X_m(a) = X_m'(a) = 0$	$Y_n(b) = Y_n'(b) = 0$		
	$X_m''(a) = X_m'''(a) = 0$	$Y_n(b) = Y_n'(b) = 0$		

()’ Denotes the derivative with respect to the corresponding coordinates where U_{mn}, V_{mn}, W_{bmn}, and W_{smn} are arbitrary parameters to be determined.

The functions $X_m(x)$ and $Y_n(y)$ are suggested by Sobhy (2013) to satisfy at least the geometric boundary conditions given in Eqs. (26) and (27), and represent approximate shapes of the deflected surface of the plate. These functions, for the different cases of boundary conditions, are listed in Table 1 noting that $\lambda = m\pi / a$ and $\mu = n\pi / b$.

Substituting expressions (28) into the governing Eqs. (24), one obtains, after some mathematical manipulations, the following equations

$$\begin{bmatrix} a_{11} & a_{12} & a_{13} & a_{14} \\ a_{21} & a_{22} & a_{23} & a_{24} \\ a_{31} & a_{32} & a_{33}-\beta N_{cr} & a_{34}-\beta N_{cr} \\ a_{41} & a_{42} & a_{43}-\beta N_{cr} & a_{44}-\beta N_{cr} \end{bmatrix} \begin{Bmatrix} U_{mn} \\ V_{mn} \\ W_{bmn} \\ W_{smn} \end{Bmatrix} = 0 \tag{29}$$

in which

$$\begin{aligned}
S_{11} &= A_{11}\alpha_{12} + A_{66}\alpha_{8} \\
S_{12} &= \left(A_{12} + A_{66}\right)\alpha_{8} \\
S_{13} &= -B_{11}\alpha_{12} - \left(B_{12} + 2B_{66}\right)\alpha_{8} \\
S_{14} &= -\left(B^{s}_{12} + 2B^{s}_{66}\right)\alpha_{8} - B^{s}_{11}\alpha_{12} \\
S_{21} &= \left(A_{12} + A_{66}\right)\alpha_{10} \\
S_{22} &= A_{22}\alpha_{4} + A_{66}\alpha_{10} \\
S_{23} &= -B_{22}\alpha_{4} - \left(B_{12} + 2B_{66}\right)\alpha_{10} \\
S_{24} &= -(B^{s}_{12} + 2B^{s}_{66})\alpha_{10} - B^{s}_{22}\alpha_{4} \\
S_{31} &= B_{11}\alpha_{13} + (B_{12} + 2B_{66})\alpha_{11} \\
S_{32} &= (B_{12} + 2B_{66})\alpha_{11} + B_{22}\alpha_{5} \\
S_{33} &= -D_{11}\alpha_{13} - 2(D_{12} + 2D_{66})\alpha_{11} - D_{22}\alpha_{5} \\
S_{34} &= -D^{s}_{11}\alpha_{13} - 2(D^{s}_{12} + 2D^{s}_{66})\alpha_{11} - D^{s}_{22}\alpha_{5} \\
S_{41} &= B^{s}_{11}\alpha_{13} + (B^{s}_{12} + 2B^{s}_{66})\alpha_{11} \\
S_{42} &= (B^{s}_{12} + 2B^{s}_{66})\alpha_{11} + B^{s}_{22}\alpha_{5} \\
S_{43} &= -D^{s}_{11}\alpha_{13} - 2(D^{s}_{12} + 2D^{s}_{66})\alpha_{11} - D^{s}_{22}\alpha_{5} \\
S_{44} &= -H^{s}_{11}\alpha_{13} - 2(H^{s}_{12} + 2H^{s}_{66})\alpha_{11} - H^{s}_{22}\alpha_{5} + \left(A^{s}_{44}\right)\alpha_{9} + \left(A^{s}_{55}\right)\alpha_{3} \\
N_{cr} &= N^{0}_{x} \\
\xi &= N^{0}_{y}/N^{0}_{x}
\end{aligned} \tag{30a}$$

with

$$\begin{aligned}
&\beta = \xi\alpha_3 + \alpha_9 \\
&(\alpha_1, \quad \alpha_3, \quad \alpha_5) = \int_0^b\int_0^a \left(X_m Y_n, \quad X_m Y_n'', \quad X_m Y_n''''\right) X_m Y_n \, dxdy \\
&(\alpha_2, \quad \alpha_4, \quad \alpha_{10}) = \int_0^b\int_0^a \left(X_m Y_n', \quad X_m Y_n''', \quad X_m'' Y_n'\right) X_m Y_n' \, dxdy \\
&(\alpha_6, \quad \alpha_8, \quad \alpha_{12}) = \int_0^b\int_0^a \left(X_m' Y_n, \quad X_m' Y_n'', \quad X_m''' Y_n\right) X_m' Y_n \, dxdy \\
&(\alpha_7, \quad \alpha_9, \quad \alpha_{11}, \quad \alpha_{13}) = \int_0^b\int_0^a \left(X_m' Y_n', \quad X_m'' Y_n, \quad X_m'' Y_n'', \quad X_m'''' Y_n\right) X_m Y_n \, dxdy
\end{aligned} \tag{30b}$$

The non-trivial solution is obtained when the determinant of Eq. (29) equals zero.

7. Buckling of FG plates under uniform temperature rise

The plate initial temperature is assumed to be T_i. The temperature is uniformly raised to a final value T_f in which the plate buckles. The temperature change is $\Delta T = T_f - T_i$. The thermal force resultant and is evaluated as

$$N_{cr} = \sum_{n=1}^{3} \int_{h_{n-1}}^{h_n} \frac{\alpha(z)E(z)(T_f - T_i)}{1-\nu} dz. \tag{31}$$

8. Buckling of FG plates under linear temperature rise

For FG plates, the temperature change is not uniform. The temperature is assumed to be varied linearly through the thickness as follows

$$T(z) = \Delta T\left(\frac{z}{h} + \frac{1}{2}\right)^{\gamma} + T_t \tag{32}$$

where the buckling temperature difference $\Delta T = T_b - T_t$ and γ is the temperature exponent $(0 \prec \gamma \prec \infty)$. Note that the value of γ equal to unity represents a linear temperature change across the thickness. While the value of γ excluding unity represents a non-linear temperature change through-the-thickness.

Similar to the previous loading case, the thermal force resultant N_{cr} is obtained by using Eqs. (32) into Eq. (31).

9. Numerical results

To illustrate the proposed approach, a ceramic-metal functionally graded sandwich plate is considered. The combination of materials consists of Titanium and Zirconia. The Young's modulus and the coefficient of thermal expansion for Titanium and Zirconia are given in Table 1.

The general approach outlined in the previous sections for the thermal buckling analysis of the FGM sandwich plates under uniform, linear, and nonlinear temperature rises through the thickness is illustrated in this section using the four variable refined plate theory.

The shear correction factor for FSDPT is set equal to 5/6. For the linear and nonlinear temperature rises through the thickness, $T_t = 25°C$.

In order to prove also the validity of the present refined plate theory, results were obtained for FGM sandwich plates under uniform, linear, and nonlinear temperature rise according to all theories. The critical buckling temperature difference $\left(T_{cr} = 10^{\ 3}\Delta T_{cr}\right)$ are considered for $p = 0,$ $2, 5, 10$ and for various types of FGM sandwich plates as is illustrated in Tables 3-5. As observed in Tables 3-5, there is a very good agreement between the present refined plate theory and other higher order plate theories. It is seen that the thermal buckling temperature increases with the increasing thickness of the FGM layers and especially for $p \geq 1$. For various power law exponent k, the thermal buckling temperature values are between those of plates made of ceramic (ZrO_2) and metal (Ti–6A1–4V). It is interesting to note that the critical buckling temperatures obtained based on CPT are noticeably greater than values obtained based on higher order shear deformation theory.

Fig. 2 shows the effect of the volume fraction index k on the thermal force resultant T_{cr} for different types of clamped square FGM sandwich plate under uniform, linear and non-linear temperature change through-the-thickness using the present four-variable refined plate theory. It is clear that the critical buckling temperature T_{cr} for the plates under a nonlinear temperature change is higher than that for the plates under uniform temperature change. While T_{cr} for the plates under linear temperature change is intermediate to the two previous thermal loading cases. It is further observed that, for the plate without core, the critical buckling T_{cr} decreases rapidly to reach minimum values and then increases gradually as the inhomogeneity parameter k increases as shown in Fig. 2(a).However, for the other sandwich FGM plates (see Figs. 2(b)-2(d)), T_{cr} decreases smoothly as k increases.

Table 2 Material properties used in the FG sandwich plate

Properties	Metal: Ti–6A1–4V	Ceramic: ZrO2
$E(GPa)$	66.2	244.27
ν	0.3	0.3
$\alpha(10^{-6}/K)$	10.3	12.766

Table 3 Critical buckling temperature T_{cr} of simply supported FGM sandwich square plates under uniform temperature rise $(a/h=5)$.

k	Theory	T_{cr}			
		1-0-1	**1-1-1**	**2-1-2**	**3-1-3**
0	CPT	3.96470	3.96470	3.96470	3.96470
	FSDPT	3.23493	3.23493	3.23493	3.23493
	SSDPT	3.23775	3.23775	3.23775	3.23775
	TSDPT	3.23652	3.23652	3.23652	3.23652
	Present	**3.23654**	**3.23654**	**3.23654**	**3.23654**
0.2	CPT	3.66606	3.65640	3.64978	3.65144
	FSDPT	3.04858	3.03637	3.03394	3.03603
	SSDPT	3.07198	3.05591	3.05598	3.05875
	TSDPT	3.07042	3.05484	3.05461	3.05729
	Present	**3.07039**	**3.05484**	**3.05458**	**3.05725**
0.5	CPT	3.34559	3.31343	3.30066	3.30593
	FSDPT	2.83507	2.80230	2.79675	2.80218
	SSDPT	2.87277	2.83331	2.83194	2.83855
	TSDPT	2.87074	2.83224	2.83030	2.83673
	Present	**2.87074**	**2.83223**	**2.83029**	**2.83673**
1	CPT	3.06734	2.96299	2.95538	2.97216
	FSDPT	2.64222	2.55161	2.55053	2.56519
	SSDPT	2.69065	2.59015	2.59458	2.61100
	TSDPT	2.68781	2.58882	2.59241	2.60856
	Present	**2.68781**	**2.58883**	**2.59241**	**2.60855**
2	CPT	2.96200	2.64806	2.68016	2.72994
	FSDPT	2.57355	2.31737	2.34734	2.38823
	SSDPT	2.63460	2.36196	2.39953	2.44337
	TSDPT	2.63018	2.36000	2.39637	2.43977
	Present	**2.63019**	**2.35999**	**2.39637**	**2.43977**
5	CPT	3.32950	2.44274	2.59922	2.73600
	FSDPT	2.86226	2.16069	2.28926	2.39882
	SSDPT	2.94205	2.21327	2.35401	2.46905
	TSDPT	2.93446	2.21009	2.34898	2.46321
	Present	**2.93443**	**2.21008**	**2.34899**	**2.46321**
10	CPT	3.82441	2.41650	2.68184	2.89384
	FSDPT	3.23289	2.14099	2.35529	2.52271
	SSDPT	3.31230	2.20150	2.42733	2.60199
	TSDPT	3.30340	2.19469	2.42186	2.59474
	Present	**3.30340**	**2.19469**	**2.42186**	**2.59476**

The variation of critical temperatures T_{cr} of clamped square FGM sandwich plates subjected to various thermal loading types are shown in Fig. 3 with respect to the side-to-thickness ratio a/h. It is seen that the critical temperature difference decreases monotonically as the side-to-thickness ratio a/h increases. Note that the critical temperatures T_{cr} of the FGM plate under uniform temperature rise is smaller than that of the plate under linear temperature rise and the latter is smaller than that of the plate under nonlinear temperature rise. Also, it is noticed that T_{cr} increases as the nonlinearity parameter γ increases.

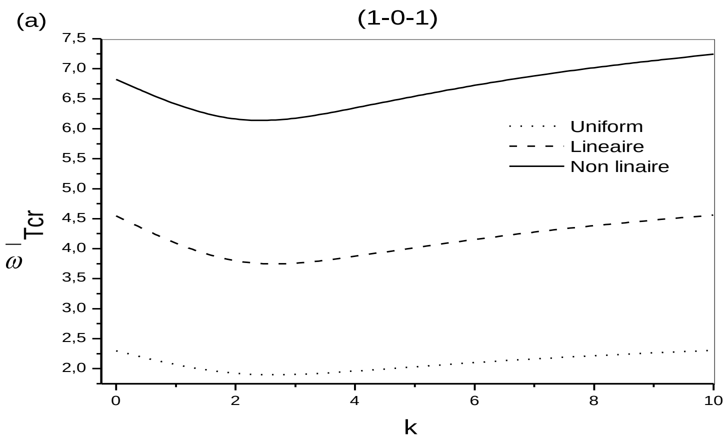

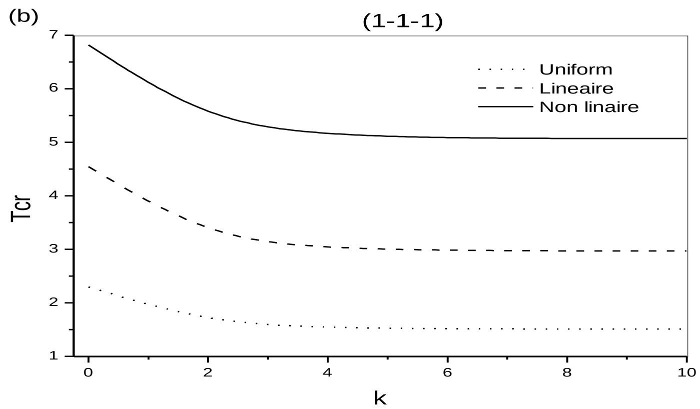

Continued-

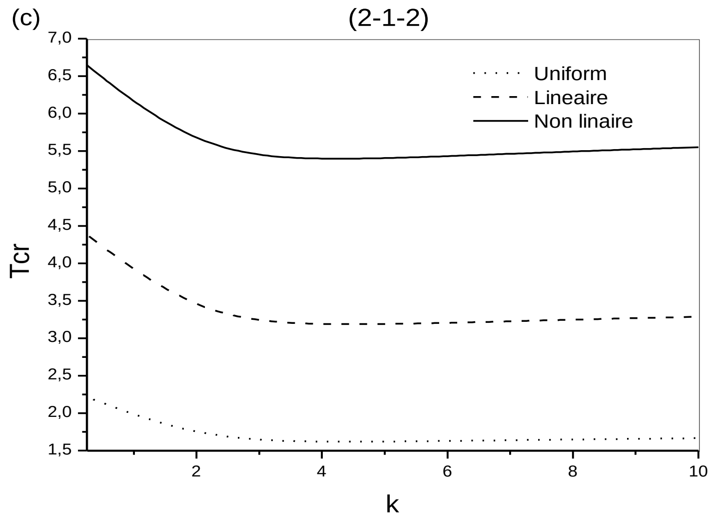

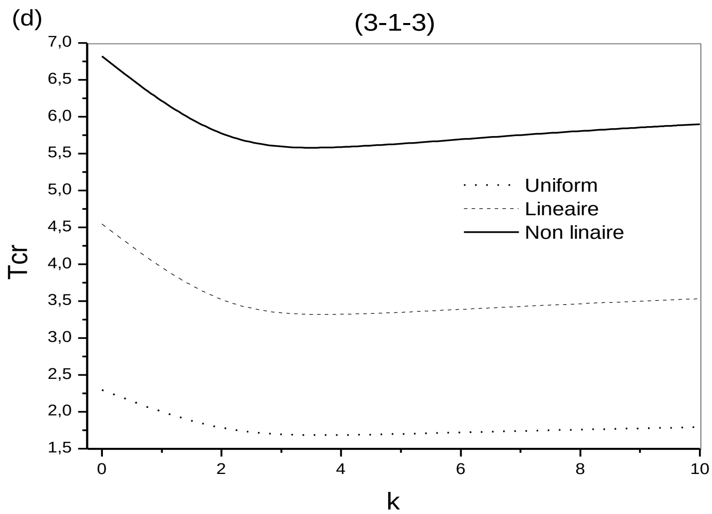

Fig. 2 Critical buckling temperature difference T_{cr} vs the power-law index k for various types of functionally graded material (FGM) sandwich clamped square plates $(a/h = 10)$: (a) the $(1 \quad 0 \quad 1)$ FGM sandwich plate, (b) the $(1 \quad 1 \quad 1)$ FGM sandwich plate, (c) the $(2 \quad 1 \quad 2)$ FGM sandwich plate, and (d) the $(3 \quad 1 \quad 3)$ FGM sandwich plate. For non-linear $\gamma = 2$

Table 4 Critical buckling temperature T_{cr} of a simply supported FGM sandwich square plates plates under linear temperature rise

k	T_{cr}				
	Theory	**1-0-1**	**1-1-1**	**2-1-2**	**3-1-3**
0	CPT	7.87940	7.87940	7.87940	7.87940
	FSDPT	6.41986	6.41986	6.41986	6.41986
	SSDPT	6.42550	6.42550	6.42550	6.42550
	TSDPT	6.42305	6.42305	6.42305	6.42305
	Present	**6.42307**	**6.42307**	**6.42307**	**6.42307**
0.2	CPT	7.28211	7.26279	7.24955	7.25287
	FSDPT	6.04716	6.02273	6.01789	6.02207
	SSDPT	6.09396	6.06183	6.06197	6.06751
	TSDPT	6.09084	6.05968	6.05922	6.06459
	Present	**6.09084**	**6.05969**	**6.05922**	**6.06457**
0.5	CPT	6.64118	6.57686	6.55131	6.56187
	FSDPT	5.62014	5.55460	5.54350	5.55435
	SSDPT	5.69554	5.61663	5.61389	5.62710
	TSDPT	5.69148	5.61449	5.61059	5.62346
	Present	**5.69144**	**5.61447**	**5.61061**	**5.62347**
1	CPT	6.08468	5.87599	5.86076	5.89431
	FSDPT	5.23443	5.05323	5.05105	5.08038
	SSDPT	5.33130	5.13030	5.13918	5.17201
	TSDPT	5.32562	5.12765	5.13482	5.16711
	Present	**5.32566**	**5.12762**	**5.13484**	**5.16709**
2	CPT	5.87400	5.24612	5.31032	5.40989
	FSDPT	5.09711	4.58475	4.64468	4.72645
	SSDPT	5.21920	4.67392	4.74908	4.83673
	TSDPT	5.21036	4.66999	4.74275	4.82954
	Present	**5.21039**	**4.66998**	**4.74277**	**4.82954**
5	CPT	6.60901	4.83549	5.14843	5.42200
	FSDPT	5.67452	4.27139	4.52851	4.74763
	SSDPT	5.83411	4.37654	4.65805	4.88811
	TSDPT	5.81891	4.37017	4.64797	4.87641
	Present	**5.81891**	**4.37019**	**4.64795**	**4.87641**
10	CPT	7.59882	4.78299	5.31369	5.73769
	FSDPT	6.41578	4.23198	4.66058	4.99542
	SSDPT	6.57459	4.35224	4.80638	5.15396
	TSDPT	6.55680	4.33937	4.79372	5.13948
	Present	**6.55682**	**4.33937**	**4.79372**	**5.13948**

Table 5 Critical buckling temperature T_{cr} of a simply supported FGM sandwich square plates plates under non-linear temperature rise $\gamma = 5$ and $(a/h = 5)$.

k	T_{cr}				
	Theory	**1-0-1**	**1-1-1**	**2-1-2**	**3-1-3**
0	CPT	23.63820	23.63820	23.63820	23.63820
	FSDPT	19.25957	19.25957	19.25957	19.25957
	SSDPT	19.27651	19.27651	19.27651	19.27651
	TSDPT	19.26915	19.26915	19.26915	19.26915
	Present	19.26904	19.26904	19.26904	19.26904
0.2	CPT	24.58692	24.34093	24.43703	24.47887
	FSDPT	20.41729	20.18492	20.28528	20.32483
	SSDPT	20.57531	20.31595	20.43388	20.47819
	TSDPT	20.56479	20.30876	20.42463	20.46833
	Present	20.56459	20.30887	20.42463	20.46807
0.5	CPT	25.21986	24.74530	2491598	24.99617
	FSDPT	21.34246	20.89907	21.08307	21.15824
	SSDPT	21.62878	21.13244	21.35073	21.43534
	TSDPT	21.61337	21.12438	21.33822	21.42148
	Present	21.61331	21.12453	21.33821	21.42153
1	CPT	25.60494	24.85771	25.09061	25.21549
	FSDPT	22.02700	21.37713	21.62417	21.73355
	SSDPT	22.43462	21.70318	22.00140	22.12553
	TSDPT	22.41074	21.69196	21.98279	22.10459
	Present	22.41079	21.69199	21.98269	22.10458
2	CPT	25.96247	24.69501	25.02775	25.23797
	FSDPT	22.52869	21.58175	21.89055	22.04964
	SSDPT	23.06831	22.00152	22.38252	22.56412
	TSDPT	23.02926	21.98304	22.35275	22.53055
	Present	23.02926	21.98310	22.35272	22.53058
5	CPT	26.92893	24.41235	25.04991	25.47341
	FSDPT	23.12129	21.56445	22.03367	22.30513
	SSDPT	23.77153	22.09533	22.66384	22.96510
	TSDPT	23.70963	22.06317	22.61489	22.91015
	Present	23.70956	22.06303	22.61498	22.91029
10	CPT	27.82720	24.36712	25.28770	25.87769
	FSDPT	23.49484	21.55996	22.17958	22.52996
	SSDPT	24.07633	22.17208	22.86373	23.24502
	TSDPT	24.01127	22.10708	22.81317	23.17972
	Present	24.01122	22.10699	22.81307	23.17970

Fig. 4 shows the effects of the aspect ratio b/a on the critical buckling temperature change T_{cr} of clamped FGM sandwich plates under various thermal loading types. It is seen that, regardless of the sandwich plate types, the critical buckling T_{cr} decreases gradually with the increase of the plate aspect ratio b/a wherever the loading type is. It is also noticed from Figure 3 that the Tcr increases with the increase of the nonlinearity parameter γ.

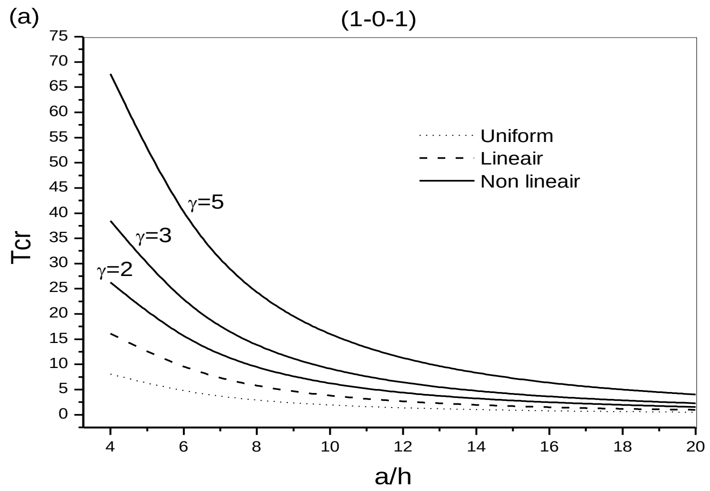

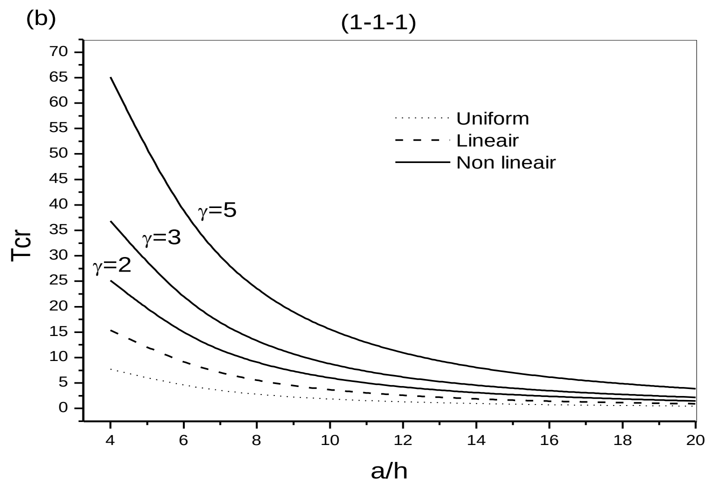

Continued-

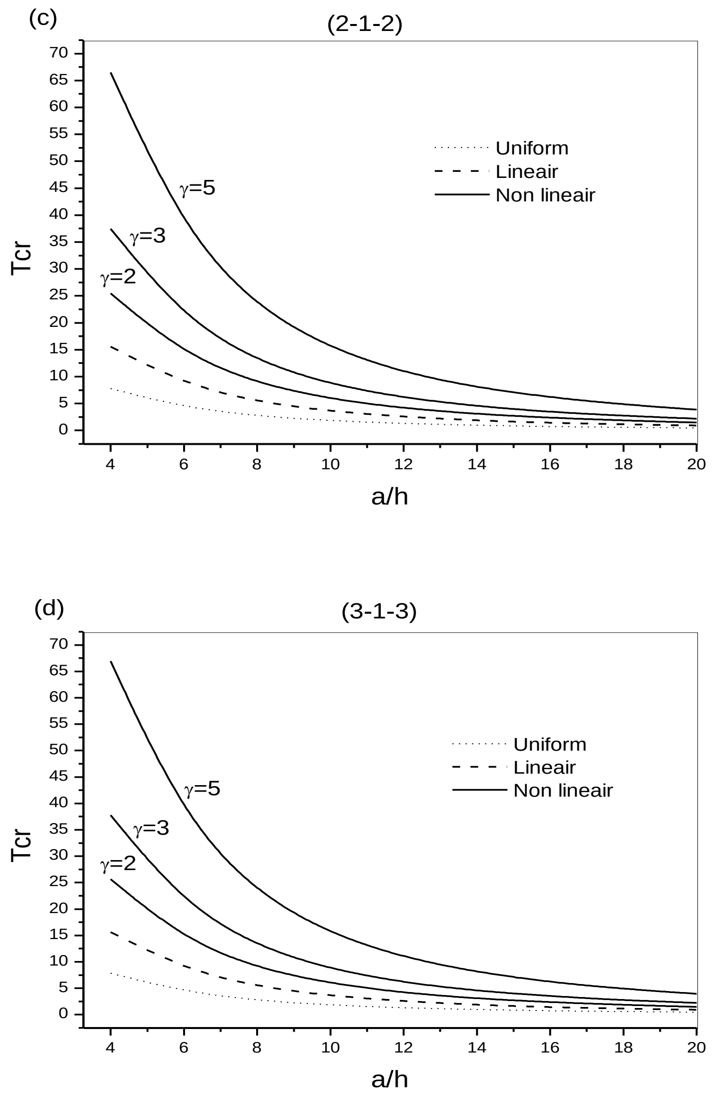

Fig. 3 Critical buckling temperature difference T_{cr} vs the side-to-thickness ratio a/h for various types of FGM sandwich clamped square plates $(k=1)$: (a) the $(1 \quad 0 \quad 1)$ FGM sandwich plate, (b) the $(1 \quad 1 \quad 1)$ FGM sandwich plate, (c) the $(2 \quad 1 \quad 2)$ FGM sandwich plate, and (d) the $(3 \quad 1 \quad 3)$ FGM sandwich plate

10. Parametric investigations

Because the functionally graded rectangular sandwich plate under assumed thermal forces and with simply supported boundary conditions bends not buckle, it is reasonable to consider only in this section the case of a sandwich plate with clamped boundary conditions (CCCC).

In this parametric study, the general approach outlined in the previous sections for thermal buckling of FGM sandwich plate with clamped boundary conditions (CCCC) has been illustrated through numerical examples.

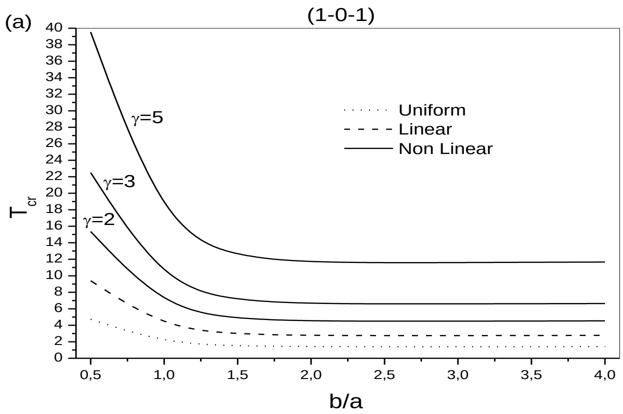

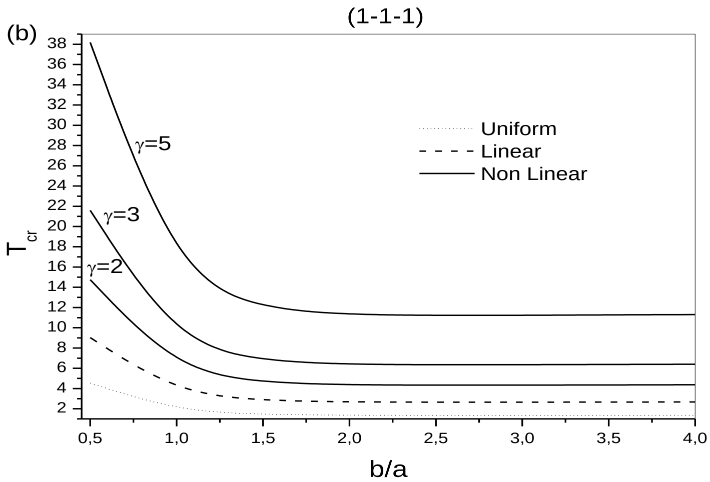

Continued-

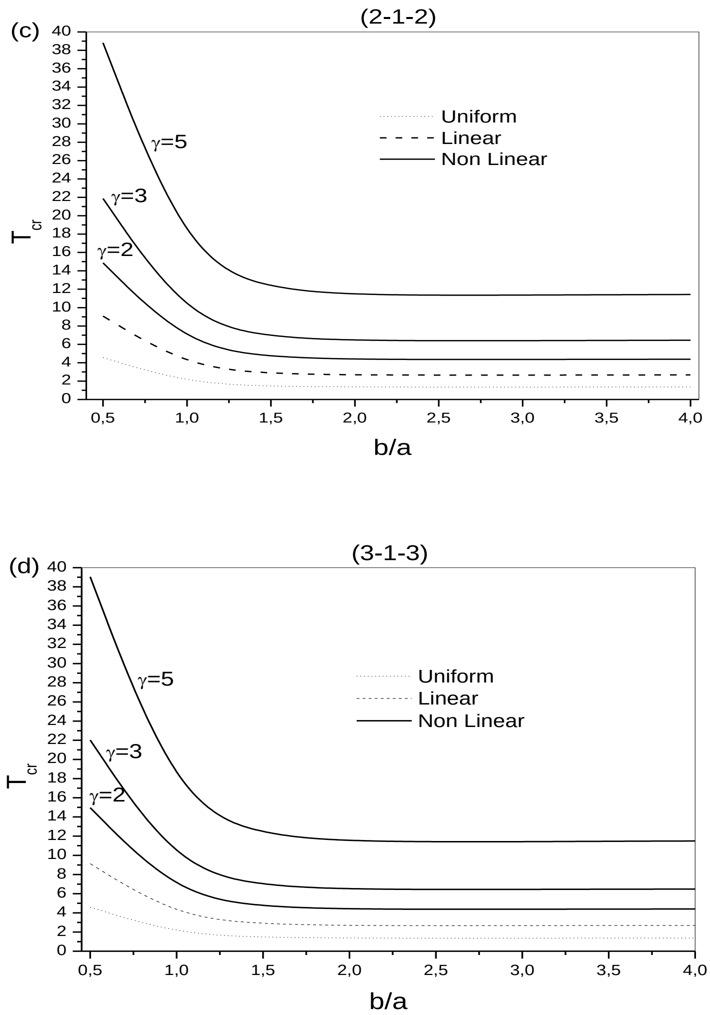

Fig. 4 Critical buckling temperature difference T_{cr} vs the plate aspect ratio b/a for various types of FGM sandwich clamped plates $(k=1, a/h=10)$: (a) the $(1 \quad 0 \quad 1)$ FGM sandwich plate, (b) the $(1 \quad 1 \quad 1)$ FGM sandwich plate, (c) the $(2 \quad 1 \quad 2)$ FGM sandwich plate, and (d) the $(3 \quad 1 \quad 3)$ FGM sandwich plate

Tables 6 and 7 exhibit the thermal force resultant T_{cr} for different values of the aspect ratio a/b, the temperature exponent and the power law index k under non-linear temperature loads at $a/h=10$ and 20, respectively. The nonlinearity temperature exponent is taken here as 2, 5, and 10.

Table 6 Critical buckling temperature T_{cr} of $(1 \quad 1 \quad 1)$ clamped FGM sandwich plates under non-linear temperature rise for different values of index k, aspect ratio a/b, and temperature exponent $(a/h=10)$.

	$a/b=1$			$a/b=2$			$a/b=3$		
	$\gamma=2$	$\gamma=5$	$\gamma=10$	$\gamma=2$	$\gamma=5$	$\gamma=10$	$\gamma=2$	$\gamma=5$	$\gamma=10$
$k=0$	6.8196	13.6392	25.0079	16.1553	32.3196	59.2291	26.3366	52.6613	96.6074
$k=0.5$	6.2284	14.7407	32.3644	15.4609	36.5878	80.3265	26.5299	62.8141	137.8929
$k=1$	5.8065	15.0311	35.9797	14.7528	38.1915	91.4186	26.0190	67.3533	161.2391
$k=1.5$	5.5465	15.1145	37.5954	14.2867	38.9263	96.8358	25.6283	69.8179	173.6483
$k=2$	5.3839	15.1332	38.2026	13.9879	39.3158	99.2407	25.3514	71.2838	179.9581
$k=2.5$	5.2799	15.1335	38.3353	13.7952	39.5356	100.1528	25.1872	72.1845	182.8339
$k=3$	5.2118	15.1281	38.2581	13.6705	39.6814	100.3539	25.0816	72.7937	184.0739
$k=3.5$	5.1659	15.1218	38.0957	13.5884	39.7844	100.2058	25.0196	73.2352	184.5526
$k=5$	5.0980	15.1124	36.4154	13.4757	39.9522	99.2061	24.9784	74.0240	183.7963

Table 7 Critical buckling temperature T_{cr} of $(1 \quad 1 \quad 1)$ clamped FGM sandwich plates under non-linear temperature rise for different values of index k, aspect ratio a/b, and temperature exponent $(a/h=20)$.

	$a/b=1$			$a/b=2$			$a/b=3$		
	$\gamma=2$	$\gamma=5$	$\gamma=10$	$\gamma=2$	$\gamma=5$	$\gamma=10$	$\gamma=2$	$\gamma=5$	$\gamma=10$
$k=0$	1.8354	3.6708	6.7296	5.1898	10.3796	19.0323	10.4051	20.8102	38.0932
$k=0.5$	1.6278	3.8528	8.4596	4.6995	11.1292	24.4312	9.6656	22.8458	50.3484
$k=1$	1.4935	3.8682	9.2605	4.3659	11.3101	27.0502	9.1152	23.5889	56.4331
$k=1.5$	1.4143	3.8546	9.5870	4.1587	11.3284	28.1749	8.7582	23.8403	59.3164
$k=2$	1.3651	3.8358	9.6858	4.0294	11.3232	28.5933	8.5180	23.9319	60.4205
$k=2.5$	1.3334	3.8214	9.6812	3.9482	11.3178	28.6707	8.3867	23.9810	60.8417
$k=3$	1.3126	3.8110	9.6367	3.8954	11.3039	28.5818	8.2878	24.0388	60.6596
$k=3.5$	1.2988	3.8017	9.5778	3.8607	11.2951	28.4453	8.2085	24.0229	60.6473
$k=5$	1.2777	3.7880	9.4059	3.8061	11.2766	27.9945	8.1192	24.0628	59.6594

It can be seen that as the power law index k increases, the thermal force resultant T_{cr} decreases to reach lowest values only for the case when $\gamma = 2$.
For the case of $\gamma = 5$ and 10, as the power law index k increases, the thermal force resultant T_{cr} increases to reach larger values and then decreases.
it is noticed that T_{cr} increases as the nonlinearity index increases.

11. Conclusions

In the present study, thermal buckling behavior of functionally graded sandwich plates with clamped boundary conditions and subjected to uniform, linear and non-linear temperature rises across the thickness direction has been investigated. The theory accounts for a quadratic variation of the transverse shear strains across the thickness, and satisfies the zero traction boundary conditions on the top and bottom surfaces of the plate without using shear correction factors.

The accuracy of the present theory is ascertained by comparing it with other higher-order shear deformation theories where an excellent agreement was observed in all cases. Furthermore, the influences of plate parameters such as power law index, aspect ratio, the side to thickness ratio and thermal loading types on the thermal force resultant of FG sandwich plate have been comprehensively investigated.

References

Ait Amar Meziane, M., Abdelaziz, H.H. and Tounsi, A. (2014), “An efficient and simple refined theory for buckling and free vibration of exponentially graded sandwich plates under various boundary conditions”, *J. Sandw. Struct. Mater*., **16**(3), 293-318.

Ait Yahia, S., Ait Atmane, H., Houari, M.S.A. and Tounsi, A. (2015), “Wave propagation in functionally graded plates with porosities using various higher-order shear deformation plate theories”, *Struct. Eng. Mech.*, **53**(6), 1143-1165.

Attia, A., Tounsi, A., Adda Bedia, E.A. and Mahmoud, S.R. (2015), “Free vibration analysis of functionally graded plates with temperature-dependent properties using various four variable refined plate theories”, *Steel Compos. Struct.*, **18**(1), 187-212.

Belabed, Z., Houari, M.S.A., Tounsi, A., Mahmoud, S.R. and Anwar Bég, O. (2014), “An efficient and simple higher order shear and normal deformation theory for functionally graded material (FGM) plates”, *Composites: Part B*, **60**, 274-283.

Bellifa, H., Benrahou, K.H., Hadji, L., Houari, M.S.A. and Tounsi, A. (2016), “Bending and free vibration analysis of functionally graded plates using a simple shear deformation theory and the concept the neutral surface position”, *J. Braz. Soc. Mech. Sci. Eng.*, **38**, 265-275.

Bennoun, M., Houari, M.S.A. and Tounsi, A. (2016), “A novel five variable refined plate theory for vibration analysis of functionally graded sandwich plates”, *Mech. Adv. Mater. Struct*., **23**(4), 423 – 431.

Bouchafa, A., Bachir Bouiadjra, M., Houari, M.S.A. and Tounsi, A. (2015), “Thermal stresses and deflections of functionally graded sandwich plates using a new refined hyperbolic shear deformation theory”, *Steel Compos. Struct.*, **18**(6), 1493-1515.

Bouderba, B., Houari, M.S.A. and Tounsi, A. (2013) “Thermomechanical bending response of FGM thick plates resting on Winkler–Pasternak elastic foundations”, *Steel Compos. Struct*., **14**(1), 85-104.

Bouiadjra, M.B., Houari, M.S.A. and Tounsi, A. (2012), “Thermal buckling of functionally graded plates according to a four-variable refined plate theory”, *J. Therm. Stresses*, **35**, 677-694.

Bousahla, A.A., Houari, M.S.A., Tounsi, A. and Adda Bedia, E.A. (2014), “A novel higher order shear and normal deformation theory based on neutral surface position for bending analysis of advanced composite plates”, *Int. J. Comput. Meth*., **11**(6), 1350082.

Bourada, M., Kaci, A., Houari, M.S.A. and Tounsi, A. (2015), "A new simple shear and normal deformations theory for functionally graded beams", *Steel Compos. Struct.*, **18**(2), 409-423.

El-Hadek, M. and Tippur, H.V. (2003), "Dynamic fracture parameters and constraint effects in functionally graded syntactic epoxy foams", *Int. J. Solids Struct.*, **40**, 1885-1906.

Fukui, Y. (1991), "Fundamental investigation of functionally gradient material manufacturing system using centrifugal force", *Int. J. Japanese Soci. Mech. Eng.*, **3**, 144-148.

Fukui, Y., Yamanaka, N. and Enokida, Y. (1997), "Bending strength of an AI-AI3Ni functionally graded material", *Composites: Part B*, **28** B, 37-43.

Hamidi, A., Houari, M.S.A., Mahmoud, S.R. and Tounsi, A. (2015), "A sinusoidal plate theory with 5-unknowns and stretching effect for thermomechanical bending of functionally graded sandwich plates", *Steel Compos. Struct.*, **18**(1), 235-253.

Hebali *et al.* (2014), "A new quasi-3D hyperbolic shear deformation theory for the static and free vibration analysis of functionally graded plates", *J. Eng. Mech. - ASCE*, **140**, 374-383.

Javaheri, R. and Eslami, M.R. (2002), "Buckling of functionally graded plates under in-plane compressive loading", *ZAMM*, **82**(4), 277-283.

Javaheri, R. and Eslami, M.R. (2002), "Thermal buckling of functionally graded plates", *AIAA*, **40**(1), 162-169.

Javaheri, R., and Eslami, M. R., (2002), "Thermal Buckling of Functionally Graded Plates Based on Higher Order Theory", *J. Therm. Stress*, **25**(1), 603–625.

Koizumi, M. (1997), "FGM Activites in Japan", *Composite: Part B*, Vol. **28**(1), 1-4.

Mahi, A., Adda Bedia, E.A. and Tounsi, A. (2015), "A new hyperbolic shear deformation theory for bending and free vibration analysis of isotropic, functionally graded, sandwich and laminated composite plates", *Appl. Math. Modell.*, **39**, 2489-2508.

Samsam, B.A. and Eslami, M.R. (2005), "Buckling of imperfect functionally graded plates under in-plane compressive loading", *Thin. Wall. Struct.*, **43**, 1020-1036.

Samsam, B.A. and Eslami, M.R. (2005), "Effect of initial imperfection on thermal buckling of functionally graded plates", *J. Therm. Stress*, **28**, 1183-1198.

Samsam, B. A. and Eslami, M. R. (2006), "Thermal buckling of imperfect functionally graded plates", *Int. J. Solids Struct.*, **43**, 4082-4096.

Samsam, B.A. and Eslami, M.R. (2007), "Buckling of Thick Functionally Graded Plates under Mechanical and Thermal Loads", *Compos. Struct*, **78**, 433-439.

Sobhy, M. (2013), "Buckling and free vibration of exponentially graded sandwich plates resting on elastic foundations under various boundary conditions", *Compos. Struct.*, **99**, 76-87.

Sohn, K.J. and Kim, J.H. (2008), "Structural stability of functionally graded panels subjected to aero-thermal loads", *Compos. Struct.*, **82**, 317-325.

Tounsi, A., Houari, M.S.A., Benyoucef, S. and Adda Bedia, E.A. (2013), "A refined trigonometric shear deformation theory for thermoelastic bending of functionally graded sandwich plates", *Aerospace Sci. Technol.*, **24**, 209-220.

Xiang, S. and Kang, G.W. (2013), "A nth-order shear deformation theory for the bending analysis on the functionally graded plates", *Eur. J. Mech. A Solids*, **37**, 336-343.

Yamanouchi, M., Koizumi, M. and Shiota, I. (1990), *Proceedings of the 1st Int. Symp. Functionally Gradient Materials*, Sendai, Japan.

Zenkour A.M. and Mashat, D.S. (2010), "Thermal buckling analysis of ceramic-metal functionally graded plates", *Nat. Sci*, **2**, 968-978.

Zidi, M., Tounsi, A., Houari, M.S.A., Adda Bedia, E.A. and Anwar Bég, O. (2014), "Bending analysis of FGM plates under hygro-thermo-mechanical loading using a four variable refined plate theory", *Aerospace Sci. Technol.*, **34**, 24-34.

CC